AD-A184 983 SELF-CONSISTENT FIELD MODEL FOR THE COMPLEX CAVITY GYROTRON(U) NAVAL RESEARCH LAB WASHINGTON DC A W FLIFLET ET AL. 17 SEP 87 NRL-MR-5881 1/1

UNCLASSIFIED F/G 14/2 NL

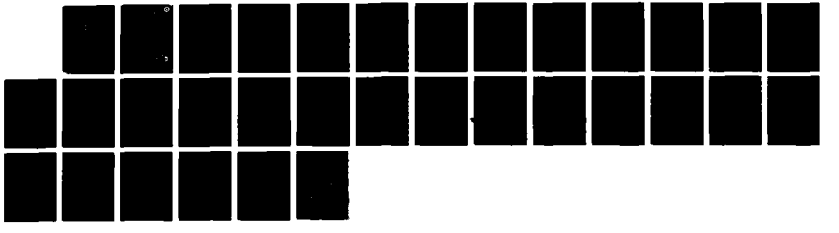

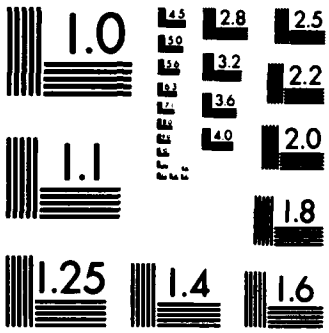

MICROCOPY RESOLUTION TEST CHART
NATIONAL BUREAU OF STANDARDS-1963-A

Naval Research Laboratory

Washington, DC 20375-5000 NRL Memorandum Report 0000 Date 1986

DTIC FILE COPY

NRL Memorandum Report 5881

AD-A184 983

Self-Consistent Field Model for the Complex Cavity Gyrotron

A. W. FLIFLET, R. C. LEE* AND M. E. READ

High Power Electromagnetic Radiation Branch
Plasma Physics Division

**JAYCOR, Inc.*
Alexandria, VA 22304

September 17, 1987

DTIC ELECTE SEP 2 5 1987 S D E

Approved for public release; distribution unlimited.

87 9 18 001

SECURITY CLASSIFICATION OF THIS PAGE

REPORT DOCUMENTATION PAGE

1a. REPORT SECURITY CLASSIFICATION UNCLASSIFIED	1b. RESTRICTIVE MARKINGS
2a. SECURITY CLASSIFICATION AUTHORITY	3 DISTRIBUTION / AVAILABILITY OF REPORT Approved for public release; distribution unlimited.
2b. DECLASSIFICATION / DOWNGRADING SCHEDULE	
4. PERFORMING ORGANIZATION REPORT NUMBER(S) NRL Memorandum Report 5881	5. MONITORING ORGANIZATION REPORT NUMBER(S)
6a. NAME OF PERFORMING ORGANIZATION Naval Research Laboratory 6b. OFFICE SYMBOL (If applicable) Code 4740	7a. NAME OF MONITORING ORGANIZATION
6c. ADDRESS (City, State, and ZIP Code) Washington, DC 20375-5000	7b. ADDRESS (City, State, and ZIP Code)
8a. NAME OF FUNDING / SPONSORING ORGANIZATION DOE and ONR 8b. OFFICE SYMBOL (If applicable)	9. PROCUREMENT INSTRUMENT IDENTIFICATION NUMBER
8c. ADDRESS (City, State, and ZIP Code) Washington, DC 20545 Washington, DC 20305	10. SOURCE OF FUNDING NUMBERS PROGRAM ELEMENT NO. / PROJECT NO. / TASK NO. (See page ii) / WORK UNIT ACCESSION NO.

11. TITLE (Include Security Classification)

Self-Consistent Field Model for the Complex Cavity Gyrotron

12. PERSONAL AUTHOR(S) Fliflet, A. W., Lee, R. C.* and Read, M. E.

13a. TYPE OF REPORT	13b. TIME COVERED	14. DATE OF REPORT (Year, Month, Day)	15. PAGE COUNT
Interim	FROM 1/83 TO 6/86	17 September 1987	32

16. SUPPLEMENTARY NOTATION

*JAYCOR, Inc., Alexandria, VA 22304

17. COSATI CODES		
FIELD	GROUP	SUB-GROUP

18. SUBJECT TERMS (Continue on reverse if necessary and identify by block number)
Gyrotron oscillator Mode selection
Millimeter wave sources "Complex" or "step-cavities"
(Continues)

19. ABSTRACT (Continue on reverse if necessary and identify by block number)

Mode competition in gyrotrons with highly overmoded cavities can degrade efficiency and output mode purity. One approach to mode selection which has been demonstrated experimentally involves a sudden change in the cavity radius. Cavities with this feature are called "complex-" or "step-cavities". This paper presents a theoretical model for the step-cavity gyrotron. The model applied to steady state operation. The axial variation of the cavity RF fields is determined self-consistently with the electron beam motion by integration of the wave equation simultaneously with the nonlinear electron equations of motion. The model accounts for mode conversion effects at the step as well as beam loading effects such cavity Q modification and frequency pulling. The model is applied to the analysis of a TE_{01}/TE_{02} complex cavity gyrotron.

20. DISTRIBUTION / AVAILABILITY OF ABSTRACT ☑ UNCLASSIFIED/UNLIMITED ☐ SAME AS RPT. ☐ DTIC USERS	21. ABSTRACT SECURITY CLASSIFICATION UNCLASSIFIED
22a. NAME OF RESPONSIBLE INDIVIDUAL Arne W. Fliflet	22b. TELEPHONE (Include Area Code) (202) 767-2469 22c. OFFICE SYMBOL Code 4740

DD FORM 1473, 84 MAR 83 APR edition may be used until exhausted.
All other editions are obsolete.

SECURITY CLASSIFICATION OF THIS PAGE

PROGRAM ELEMENT NO.	PROJECT NO.	TASK NO.	WORK UNIT ACCESSION NO.
DOE 61153N		OPO/DC (243/2) RR011-09-41	DN780-307 DN880-061

18. SUBJECT TERMS (Continued)

Mode competition
Overmoded cavities
Step-cavity gyrotron
Enhanced stability

CONTENTS

Accession For
NTIS GRA&I [X]
DTIC TAB [ ]
Unannounced [ ]
Justification
By
Distribution/
Availability Codes
Dist | Avail and/or Special
A-1

DTIC COPY INSPECTED

SELF-CONSISTENT FIELD MODEL FOR THE COMPLEX CAVITY GYROTRON

I. INTRODUCTION

The gyrotron oscillator is currently under development as a high average power, efficient millimeter wave source. The gyrotron derives much of its high power capability from the ability to operate stably in a single mode of an over-moded resonator. However, as the trend toward higher output power leads to increasingly over-moded cavities, the mode density increases and mode competition can occur. This effect can seriously degrade the efficiency of operation and is undesirable for other reasons as well. For example, the plasma heating application for magnetic fusion involves highly mode and frequency specific transmission systems for the output power. Thus mode selection techniques for gyrotron cavities are of considerable interest, particularly with respect to different transverse modes. One method which has been successfully demonstrated in several devices involves a sudden change or step in the cavity wall radius. The "complex-cavity" or "step-cavity" concept was first demonstrated in a TE_{01}/TE_{04} configuration by Carmel et al (1983), and has been incorporated in a 60 GHz TE_{01}/TE_{02} device (Felch et al 1984) and in a 140 GHz TE_{02}/TE_{03} device developed by Varian. The 60 GHz Varian device produces 200 kW of cw power and it and the 140 GHz gyrotron currently under development represent the current state-of-the-art of high average power gyrotrons in the U.S.

The essential idea of the complex cavity approach is that a particular pair of modes having the same azimuthal index m can be tightly coupled to form a high Q mode of the complete cavity. In the step cavity configuration

Manuscript approved October 17, 1987.

(Carmel et al 1983) mode coupling occurs at a sudden change in the cavity wall radius. The cavity is designed such that the local waveguide modes of this mode pair are simultaneously near cut-off in the two cylindrical sections of the cavity at the desired operating frequency. Mode pairs with a different mode index m' will not be simultaneously resonant in the cavity sections and will form modes of the complete cavity which are less favorable for gyrotron operation. Such modes may have a shorter effective interaction length, a lower Q factor, or lower inter-mode conversion efficiency at the step. These effects usually lead to higher starting currents. The success of this approach depends on several factors including mode density, fabrication tolerances, and mode conversion at the cavity step. As the mode density increases, more than one mode pair can become simultaneously resonant. Step-cavity gyrotrons are more sensitive to machining tolerances than conventional gyromonotrons because of the bimodal resonance condition. Finally, conversion into unwanted modes at the step can degrade the mode purity and Q factor of the device. Clearly, theoretical models are needed which can investgate and quantify these effects.

In this paper a theoretical model of the step-cavity gyrotron is presented. The model is based on a Self-Consistent Field theory for low Q gyromonotrons developed previously (Fliflet et al. 1982). This theory treats steady-state operation in a single cavity mode. The axial variation of the cavity RF fields is determined self-consistently with the electron beam motion by integrating the wave equation simultaneously with the electron equations of motion. The theory accounts for important aspects of gyrotron operation such as modification of the cavity Q and resonant frequency by beam loading. These effects are omitted when cold cavity eigenmodes are used to describe the RF

field distribution during operation. Calculations for step-cavity gyrotrons have to date been based on the use of cold cavity eigenmodes and it is of interest to explore beam loading effects for such devices.

In this paper, the SCF approach for gyromonotrons is extended to account for a sudden change or step in the cavity diameter. In addition to the beam loading effects noted for gyromonotrons, the method predicts the mode conversion efficiency at the step. Mode conversion at the step is calculated by the field matching technique of Masterman and Clarricoats (1971). To obtain a computationally tractable model suitable for use in design studies, the following simplifications are introduced: (1) The beam is assumed to interact with just one TE_{mn} waveguide mode in each cavity section. The modes in the two sections will differ only in radial index. (2) Non-resonant modes which may be excited at the step are assumed to propagate out of the cavity without reflection by the cavity structure. This is consistent with the fact that such modes are not close to cutoff and will be weakly affected by changes in the cavity wall radius. With these assumptions, SCF calculations for the step-cavity gyrotron are not significantly more involved than for conventional gyromonotrons. These assumptions appear to be consistent with the step cavity concept, but their validity must ultimately be tested by comparison with experiment or with more general calculations.

The method has been applied to the analysis of a TE_{01}/TE_{04} step cavity configuration similar to the NRL experiment (Carmel et al 1983). The results indicate that the selectivity of the cavity for the m=0 mode is enhanced compared to a conventional TE_{04} gyromonotron. The TE_{01} - TE_{04} mode conversion efficiency at the cavity step can be high (95%) which allows good output mode

purity. The selectivity of the cavity is optimum when the m=2 competing mode is not cut-off in the input section since in this case the Q factor for this mode is degraded by diffraction losses at the input. This effect was exploited in the NRL experiment and probably contributed signifigantly to the stability of the device. The effect of having the m=2 mode cut-off in the input section was investigated.

The remainder of this paper consists of three sections. Section II contains an outline of the self-consistent field theory and describes the present application of Masterman and Clarricoat's field matching technique for waveguide discontinuities. Section III presents the results of calculations, and Section IV contains discussion of results and our conclusions. Except as noted, MKS units are used throughout.

II. THEORETICAL MODEL

A. Self-Consistent Field Equations

The electron beam - rf field dynamics are treated according to a system of coupled, non-linear, ordinary differential equations derived previously (Fliflet et al 1982). The electrons follow helical trajectories due to a strong applied axial magnetic field which may be weakly tapered and experience perturbing rf fields. Space-charge effects are neglected. On either side of the cavity step, the beam is assumed to interact with a single TE circular waveguide mode of the form:

$$\vec{E}_t = \mathrm{Re}\{C_{mn}[k_{mn}J'_m(k_{mn}r)\hat{\theta} + imJ_m(k_{mn}r)\hat{r}/r]f(z)\exp[i(\omega t - m\theta)]\} \tag{1}$$

where ω is the wave frequency, J_m is a Bessel function of the first kind, the prime denotes differentiation, and $k_{mn} = x_{mn}/r_w$ is the transverse wave number. The normalization constant is given by

$$C_{mn} = [\sqrt{\pi(x_{mn}^2 - m^2)}\ J_m(x_{mn})]^{-1} \tag{2}$$

where x_{mn} is the nth zero of J'_m and r_w is the radius of the cavity wall which is assumed to be weakly irregular except at the step. The axial dependence of the rf fields in the resonator is given by the complex profile function

$$f(z) = f(z)\exp[-i\phi(z)] \tag{3}$$

It is convenient to use the normalized momentum variable

$$\vec{u} = \gamma\vec{v} \tag{4}$$

where $\vec{v}$ is the electron velocity and γ is the relativistic factor given by:

$$\gamma = [1 + u^2/c^2]^{1/2} \tag{5}$$

and c is the speed of light. To obtain a slow time scale formulation the transverse momentum is expressed in terms of magnitude and phase variables u_t and Λ according to

$$u_x + iu_y = iu_t \exp[i(\omega t/s - \Lambda)] \tag{6}$$

where s is the harmonic number. Consider the case of an annular electron beam propagating in a circular waveguide structure. Neglecting the interaction with the rf magnetic field components and considering the interaction with a single harmonic of the cyclotron frequency, the equations for steady-state operation are given by:

$$\frac{du_t}{dz} = -\frac{\gamma\eta C_{mn} J_{m-s}(k_{mn}R_o)}{u_z}\frac{\partial J_s(k_{mn}r_L)}{\partial r_L}\mathrm{Re}\{f\exp(is\Lambda)\} + \frac{u_t}{2B_z}\frac{dB_z}{dz} \quad (7a)$$

$$\frac{d\Lambda}{dz} = -\frac{\gamma\eta}{u_z u_t} C_{mn} J_{m-s}(k_{mn}R_o)\frac{s}{r_L} J_s(k_{mn}r_L)\mathrm{Re}\{if\exp(is\Lambda)\} + \frac{\gamma}{u_z}(\omega/s - \Omega_z/\gamma) \quad (7b)$$

$$\frac{du_z}{dz} = -\frac{u_t^2}{2u_z B_z}\frac{dB_z}{dz} \quad (7c)$$

$$\left[\frac{d^2}{dz^2} + (\omega/c)^2 - k_{mn}^2\right]f =$$

$$-2i\mu\omega I_o\, C_{mn} J_{m-s}(k_{mn}R_o)\,\frac{1}{2\pi}\int_o^{2\pi} d\Lambda_o \frac{u_t}{u_z}\frac{\partial J_s(k_{mn}r_L)}{\partial r_L}\exp(-is\Lambda) \quad (7d)$$

where z is the axial spatial coordinate, $\eta = e/m$ is the charge to rest mass ratio for an electron, and R_o is the guiding center radius for a thin annular beam. The local non-relativistic cyclotron frequency is given by

$$\Omega_z = \eta B_z \quad (8)$$

and the axial magnetic field is assumed to be constant within the electron

beam. The Larmor radius $r_L = u_t/\Omega_z$. The first three equations are derived from the Lorentz force equation, and the last equation is derived from Maxwell's equations. In Eq.(7d) I_o is the beam current and Λ_o is the electron phase entering the interaction region. Eqs.(7a-d) are solved subject to appropriate boundary conditions as discussed below.

It is readily verified that the total power flowing in the beam and interacting mode is conserved by Eqs.(7a-d).

B. Field Matching Procedure at Cavity Step

A computer oriented field matching technique due to Masterman and Clarricoats (1971) is used to treat mode conversion at the cavity step. The present application involves the junction of two coaxial circular waveguides. The discontinuity plane aperture cross section is equal to the smaller waveguide cross section. In this method the rf fields in the discontinuity plane are expressed in terms of transverse vector functions. For a TE mode the transverse electric and magnetic fields in waveguide I are in general given by

$$\vec{E}_t = \sum_m (a_{im} + a_{rm})\vec{e}_m \tag{9a}$$

$$\vec{H}_t = \sum_m (a_{im} - a_{rm})\vec{h}_m \tag{9b}$$

where the transverse vector functions are given by

$$\vec{e} = z \times \vec{\nabla}_t \psi \tag{10a}$$

$$\vec{h} = -\vec{\nabla}_t \psi \tag{10b}$$

The scalar function ψ satisfies the wave equation

$$(\nabla_t^2 + k_t^2)\,\psi = 0 \tag{11}$$

and the boundary condition

$$\frac{\partial \psi}{\partial r} = 0 \tag{12}$$

at the waveguide wall. For a circular waveguide, the scalar function is given by

$$\Psi = C_{mn} J_m(k_{t1} r) e^{-im\theta} \tag{13}$$

where $k_{t1} = x_{mn1}/r_{w1}$. The vector functions $\vec{e}$ and $\vec{h}$ satisfy the orthonormality condition

$$\int_s \vec{e}_i \times \vec{h}_j \cdot d\vec{s} = \delta_{ij} \tag{14}$$

where $\delta_{ij} = 0$ if $i \neq j$ or 1 if $i = j$. The coefficient a_{im} is the amplitude of a mode incident to the discontinuity plane, a_{rm} is the amplitude of a mode reflected from the plane. Both propagating and evanescent modes should be included. Similarly, in waveguide II the fields are given by

$$\vec{E}'_t = \sum_n (a'_{in} + a'_{rn})\vec{e}'_n \tag{15a}$$

$$\vec{H}'_t = \sum_n (a'_{rn} - a'_{in})\vec{h}'_n \tag{15b}$$

where $\vec{e}'_n$ and $\vec{h}'_n$ are vector functions for waveguide II. To proceed, the infinite series representations of the transverse fields are truncated after a finite number of terms, say, p modes in waveguide I and p′ modes in waveguide II. The transverse electric and magnetic fields must be continuous across the aperture. This condition and the orthogonality of the vector functions leads to a set of linear equations for the mode amplitudes:

$$a'_{in} + a'_{rn} = R_{nm}(a_{im} + a_{rm}) \tag{16a}$$

$$S_{mn}(a'_{rn} + a'_{in}) = a_{im} + a_{rm} \tag{16b}$$

where the summation over repeated indicies is understood and R_{nm} and S_{mn} are given by

$$R_{nm} = \frac{\int_S \vec{e}_m \times \vec{h}'_n \cdot ds}{\int_S \vec{e}'_n \times \vec{h}'_n \cdot ds} \tag{17a}$$

$$S_{nm} = \frac{\int_S \vec{e}_m \times \vec{h}'_n \cdot d\vec{s}}{\int_S \vec{e}_m \times \vec{h}_m \cdot ds} \tag{17b}$$

For circular waveguides, R_{nm} and S_{nm} involve integrals of Bessel functions. Closed form expressions for these integrals can be obtained (Gradshteyn and

Ryzhik 1965). In the present application, waveguide I corresponds to the cavity section for which the mode M is nearly cutoff and interacts with the beam; and waveguide II corresponds to the cavity section for which the mode N is nearly cutoff and interacts with the beam. Except for the step, the cavity consists of a slightly irregular waveguide structure which has little effect on modes which are far from cutoff. It is therefore assumed that any non-resonant propagating modes excited by mode conversion at the step will simply propagate out of the system without reflection at the cavity input or output sections. Therefore, the incident mode amplitudes are all zero except for a_{im} and a'_{iN}.

In the present model, the boundary conditions on the mode M are applied at the cavity input and the self-consistent field equations are integrated up to the cavity step. Only the beam interactions with the mode M are included. This integration determines the values of a_{iM} and a_{rM} since the interaction with both forward and backward waves has been included. To continue the integration of the field equations beyond the step, it is necessary to calculate the amplitude coefficients a'_{iM} and a'_{rM}. The non-zero value of a'_{iN} results from the interaction with the beam as well as from reflection from the cavity output structure. These coefficients as well as the amplitudes of other modes excited at the step are obtained as follows: Eliminating the coefficients a'_{rm} from Eqs.(18a,b) leads to

$$2S_{mn}a'_{in} = (S_{mn}R_{n'm'} - \delta_{m,m'})a_{im'} + (S_{mn}R_{n'm'} + \delta_{m,m'})a_{rm'} \quad (20)$$

Using the facts that $a_{im} = 0$, $m \neq M$, and $a_{in'} = 0$, $n \neq N$, Eq.(20) can be rewritten in the form

$$(-S_{mn'}R_{n'm'} + \delta_{m,m'})a_{rm'} + 2S_{mN}a'_{iN}$$

$$= (S_{mn'} - \delta_{m,M})a_{iM} + (S_{mn'}R_{n'M} + \delta_{m,n})a_{rM} \qquad (21)$$

Eq.(21) consists of p inhomogeneous linear equations for p unknowns and can be solved using standard matrix methods. The unknowns are the p-1 amplitudes a_{rm}, m≠M, and a'_{iN}. The remaining p′ coefficients a_{rn} are then given by

$$a'_{rn} = R_{nm}(a_{im} + a_{rm}) - a'_{in} \qquad (22)$$

To summarize, the self-consistent field approach for step-cavity gyrotrons involves integrating Eqs.(7a-d) for the mode M up to the step, applying the field matching procedure to obtain the amplitudes of modes excited by mode conversion at the step, and then integrating Eqs.(7a-d) for mode N to the cavity output region. The desired solutions are those for which the mode N satisfies outgoing wave boundary conditions at the cavity output, i.e.,

$$df_N/dz = -ik_z f_N \qquad (23)$$

where k_z is the axial wavenumber in the output waveguide. Within the assumptions of the model, the boundary conditions for the other modes are automatically satisfied by the matching procedure.

Since f_N is complex, Eq.(23) represents two conditions. Thus the solution of the self-consistent field equations for the step-cavity

configuration - as for the gyromonotron - constitutes a two dimensional eigenvalue problem. If the mode M has the form of a growing evanescent wave in the cavity input section, then for fixed beam, magnetic field, and resonator parameters the eigenfunctions correspond to discrete pairs of values for $f_M(z_0)$ and ω. These are not known a priori and must be found by a search procedure.

III. CALCULATIONS AND RESULTS

Calculatons have been carried out for a TE_{01}/TE_{04} step cavity configuration. The cavity design is shown in Figure 1. The principal competing mode pair is the TE_{21}/TE_{24} combination. The beam voltage was taken to be 70 kV and a beam pitch ratio of $\alpha = v_t/v_z = 1.5$ was used. The cavity dimensions correspond to operation at approximately 35 GHz. A step-cavity design of this type was successfully demonstrated experimentally by Carmel et al (1982) at NRL. The cavity is designed such that for the M=0 case, the resonant mode is close to cut-off in both cavity sections, whereas for the M=2 case, the resonant frequency is considerably above cut-off in the smaller cavity section. The beam drift tube of the experimental cavity was not cut-off to the TE_{21} mode which leads to diffraction losses at the input and degradation of the Q-factor for the M=2 mode. This effect is readily achieved in cavities with the smaller section resonant for the TE_{01} mode since TE_{01} and TE_{21} cut-off radii differ significantly. It is more difficult to achieve in cavities where the smaller section supports a higher order TE_{on} mode because for $n > 1$ there is much less difference in the cut-off radii for m=0 and m=2 modes.

The convergence of the field matching procedure at the step was checked by varying the number of modes retained in the expansions on each side of the step. As discussed by Masterman and Clarricoats the number of modes retained on each side should be approximately equal to the ratio of the corresponding waveguide radii. Adequate convergence was obtained using four modes on the TE_{01} side and sixteen modes on the TE_{04} side.

The axial profile of the RF field corresponding to the M=0 mode is shown in Figure 2 for typical current and magnetic field parameters. The local efficiency as a function of cavity position is also shown.

Figure 3 shows the numerically computed oscillation threshold currents for the lowest order M=0 and M=2 modes as a function of magnetic field. The optimum efficiency operating points are also indicated. The m=2 calculations assume the mode is cut-off at the cavity input and thus are relevant to higher order mode configurations such as TE_{03}/TE_{04}, etc. The threshold current curves are shifted by about 600 Gauss. This shift is much greater than that of the corresponding threshold current curves for the TE_{04} and TE_{24} modes in a gyromonotron. Unlike the gyromonotron (Carmel et al 1982), the optimum operating point of the step cavity M=0 mode is outside the M=2 threshold current curve. Thus competition between M=0 and M=2 modes should be signifigantly reduced. Note, however, that the minimum starting current of the M=2 mode is not much higher than that of the M=0 mode in the configuration analyzed. Even though the TE_{21} mode is not close to cut-off in the smaller cavity section, it is trapped by coupling to the TE_{42} mode and has significant interactions with the beam.

Figure 4 shows the efficiency vs. beam current for several values of magnetic field for the M=0 mode. The maximum calculated efficiency is about 43%. This is somewhat less than can be achieved in a well designed gyromontron (≈ 50%) for $\alpha = 1.5$ and could probably be improved by further cavity optimization.

Mode purity is an important issue for step-type cavities since conversion of operating modes into unwanted modes can occur at the step. This effect can also reduce the cavity Q-factor. The calculated mode purity at optimum efficiency is about 95%, thus mode conversion effects due to the step are small in the present design.

IV. CONCLUSIONS

The self-consistent field approach for gyromonotrons has been extended to the analysis of step cavity configurations. The approach allows the numerical calculation of the large signal efficiency, oscillation threshold currents, loaded Q factor, and mode conversion effects at the step. The method of calculation is relatively efficient - the computational effort is not greatly increased over the gyromonotron case - thus the method is suitable for use in design optimization studies of step cavity devices.

The approach has been applied to the investigation of the lowest order M=0 and M=2 modes of a configuration designed for TE_{01}/TE_{04} operation. The magnetic fields values for optimum effiency operation are found to be more separated than in a gyromonotron, thus the competition between these modes

should be reduced. However, the minimum starting currents for the M=0 and M=2 modes are found to be comparable in the case that the TE_{21} mode is cut-off in the electron beam drift tube. It is concluded that a sufficiently large amplitude TE_{21} mode can contribute significantly to beam bunching even when not close to the cut-off condition. This can occur in step-cavity configurations when the lower order competing mode (TE_{21}) is cut-off at the cavity input and tightly coupled to the higher order mode (TE_{24}). Selectivity against the M=2 mode is considerably enhanced when the TE_{21} mode is not cut-off in the beam drift tube since in this case the overall cavity Q factor for the M=2 mode is significantly reduced and, furthermore, the TE_{21} mode does not achieve a large amplitude from being trapped. It is argued that this should be a general feature of step cavity designs. To our knowledge this effect has not been pointed out before.

The calculations show that conversion into unwanted modes at the step is small under optimum efficiency operating conditions, of order 95%.

V. ACKNOWLEDGEMENTS

We would like to acknowledge helpful discussions with Dr. John Burke. This work was supported by the Department of Energy, Contract Number DEAI01-80-ER52065, and by the Office of Naval Research.

REFERENCES

Carmel, Y., Chu, K. R., Dialetis, D., Fliflet, A. W., Read, M. E., Kim, K. J., Arfin, B., and Granatstein, V. L., 1982, Mode competition, suppression, and efficiency enhancement in overmoded gyrotron oscillators. Int. J. Infrared and Millimeter Waves, 3, 645-665.

Carmel, Y., Chu, K. R., Read, R., Ganguly, A. K., Dialetis, D., Seeley, R., Levine, J. S., and Granatstein, V. L., 1983, Realization of a highly stable and efficient gyrotron for controlled fusion research. Phys. Rev. Lett., 50, 112-116.

Felch, K. L., Bier, R., Fox, L., Huey, H., Ives, L., Jory, H., Lopez, N., Manca, J., Shively, J., Spang, S., 1984, A 60 GHz, 200 kW cw gyrotron with a pure output mode. Int. J. Electronics, 57, 815-820.

Fliflet, A. W., Read, M. E., Chu, K. R., Seeley, R., 1982, A self-consistent field theory for gyrotron oscillators: application to a low Q gyromontron. Int. J. Electronics, 53, 505-521.

Gradsteyn, I. S., and Ryzhik, I. W., 1965, Table of Integrals, Series, and Products (Academic, New York), 5.54, p.634.

Masterman, P. H., and Clarricoats, P. J. B., 1971, Computer field-matching solution of waveguide transverse discontinuities. Proc. IEE, 118, 51-63.

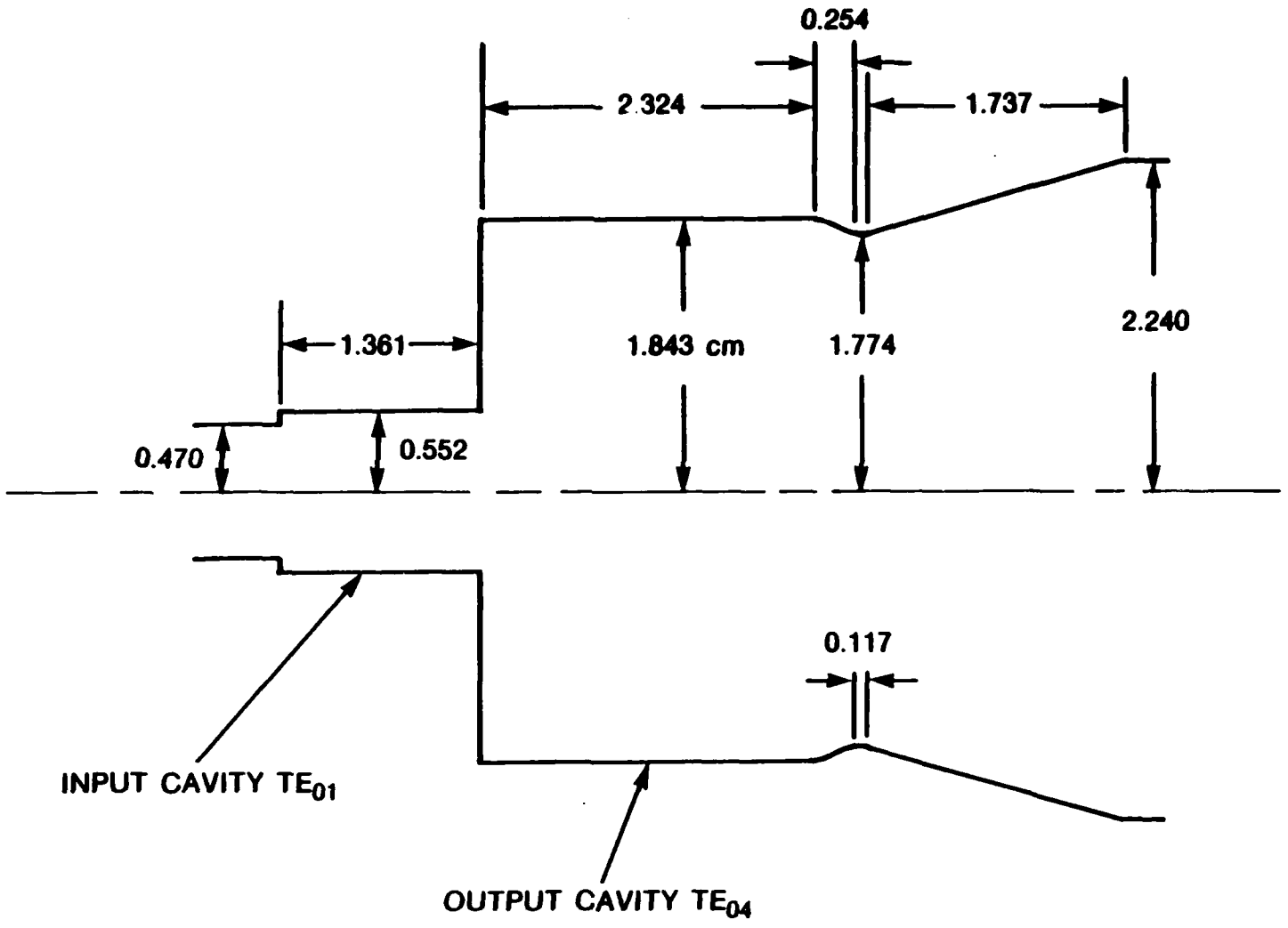

Figure 1. 35 GHz TE_{01}/TE_{04} step-cavity design used in calculations.

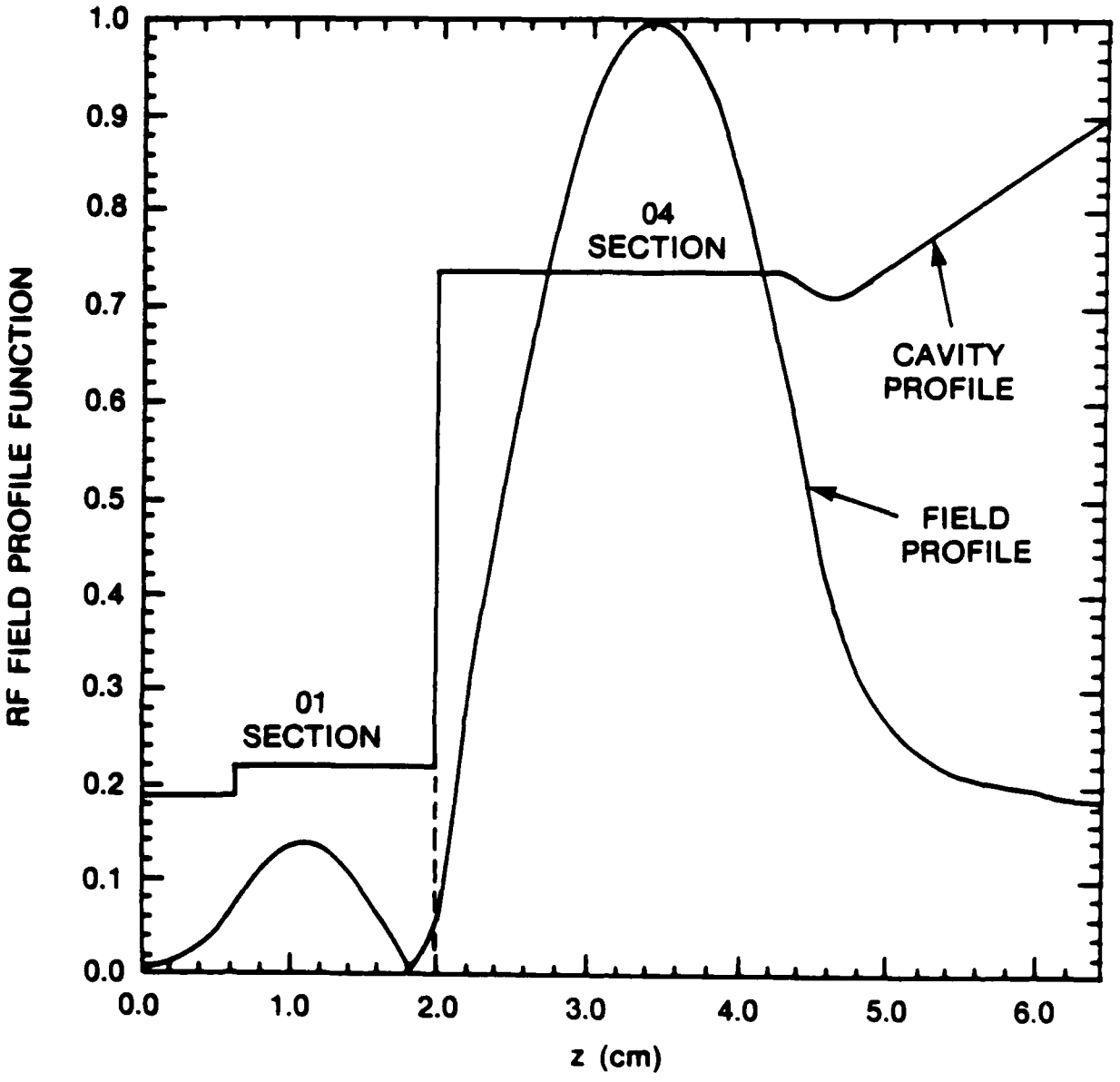

Figure 2. Axial RF field profile for M=0 mode corresponding to optimum efficiency conditions.

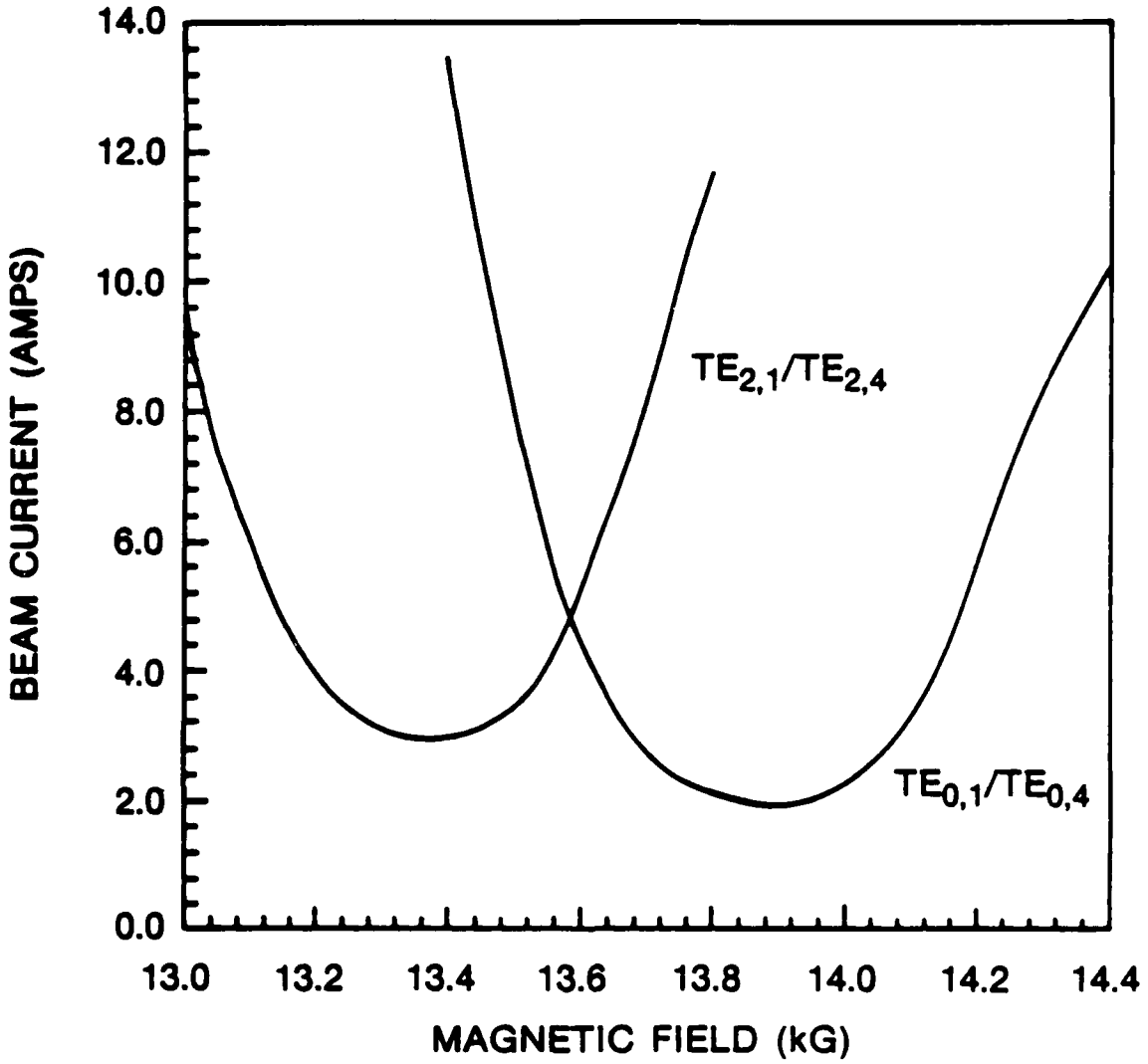

Figure 3. Oscillation threshold currents for for lowest order M=0 and M=2 modes as a function of magnetic field.

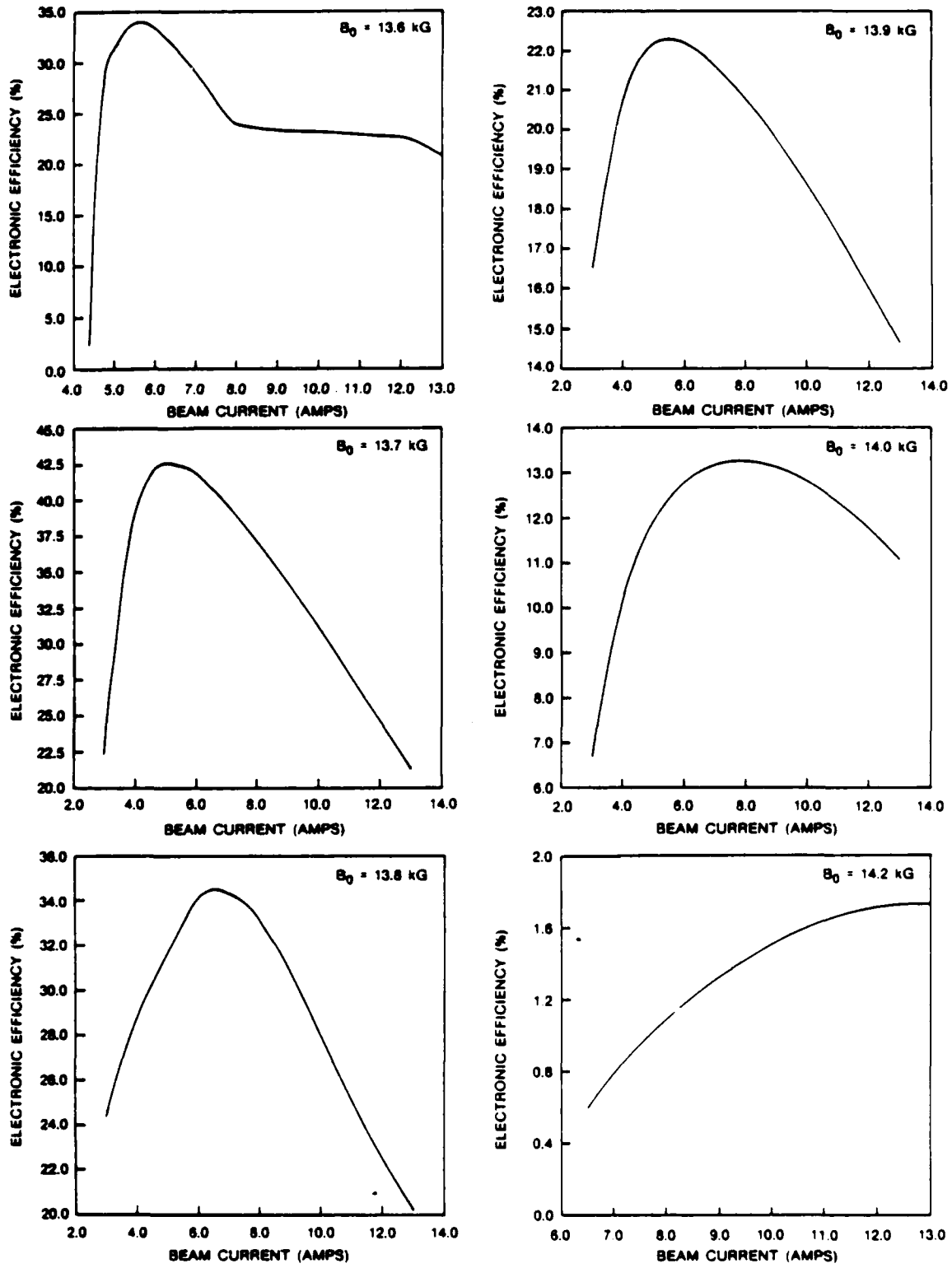

Figure 4. Nonlinear efficiency vs. beam current for the lowest order M=0 mode at several values of magnetic field.

DISTRIBUTION LIST

Air Force Avionics Laboratory
AFWAL/AADM-1
Wright/Patterson AFB, Ohio 45433
Attn: Walter Friez — 1 copy

Air Force Office of
Scientific Research
Bolling AFB
Washington, D.C. 20332
Attn: H. Schlossberg — 1 copy

Air Force Weapons Lab
Kirkland AFB
Albuquerque, New Mexico 87117
Attn: Dr. William Baker — 1 copy

Columbia University
520 West 120th Street
Department of Electrical Engineering
New York, N.Y. 10027
Attn: Dr. S.P. Schlesinger — 1 copy

Columbia University
520 West 120th Street
Department of Applied Physics
and Nuclear Engineering
New York, New York 10027
Attn: T.C. Marshall — 1 copy

Cornell University
School of Applied and Engineering Physics
Ithica, New York 14853
Attn: Prof. Hans H. Fleischmann — 1 copy
John Nation — 1 copy
R. N. Sudan — 1 copy

Dartmouth College
18 Wilder, Box 6127
Hanover, New Hampshire 03755
Attn: Dr. John E. Walsh — 1 copy

Department of Energy
Washington, D.C. 20545
Attn: C. Finfgeld/ER-542, GTN — 1 copy
T.V. George/ER-531, GTN — 1 copy
D. Crandall/ER-55, GTN — 1 copy

Defense Advanced Research Project Agency/DEO
1400 Wilson Blvd.
Arlington, Virginia 22209
Attn: Dr. S. Shey — 1 copy
Dr. L. Buchanan — 1 copy

Defense Communications Agency
Washington, D.C. 20305
Attn: Dr. Pravin C. Jain
Assistant for Communications
Technology — 1 copy

Defense Nuclear Agency
Washington, D.C. 20305
Attn: Mr. J. Farber — 1 copy
Maj. J. Benson — 1 copy
Capt. D. Stone — 1 copy
Mr. Lloyd Stossell — 1 copy

Defense Technical Information Center
Cameron Station
5010 Duke Street
Alexandria, Virginia 22314 — 2 copies

Georgia Tech. EES-EOD
Baker Building
Atlanta, Georgia 30332
Attn: Dr. James J. Gallagher — 1 copy

Hanscomb Air Force Base
Stop 21, Massachusetts 01731
Attn: Lt. Rich Nielson/ESD/INK — 1 copy

Hughes Aircraft Co.
Electron Dynamics Division
3100 West Lomita Boulevard
Torrance, California 90509
Attn: J. Christiansen — 1 copy
J.J. Tancredi — 1 copy

KMS Fusion, Inc.
3941 Research Park Dr.
P.O. Box 1567
Ann Arbor, Michigan 48106
Attn: S.B. Segall — 1 copy

Lawrence Livermore National Laboratory
P.O. Box 808
Livermore, California 94550
Attn: Dr. D. Prosnitz — 1 copy
Dr. T.J. Orzechowski — 1 copy
Dr. J. Chase — 1 copy

Los Alamos Scientific Laboratory
P.O. Box 1663, AT5-827
Los Alamos, New Mexico 87545

Attn:	Dr. J.C. Goldstein	1 copy
	Dr. T.J.T. Kwan	1 copy
	Dr. L. Thode	1 copy
	Dr. C. Brau	1 copy
	Dr. R. R. Bartsch	1 copy

Massachusetts Institute of Technology
Department of Physics
Cambridge, Massachusetts 02139

Attn:	Dr. G. Bekefi/36-213	1 copy
	Dr. M. Porkolab/NW 36-213	1 copy
	Dr. R. Davidson/NW 16-206	1 copy
	Dr. A. Bers/NW 38-260	1 copy
	Dr. K. Kreischer	1 copy

Massachusetts Institute of Technology
167 Albany St., N.W. 16-200
Cambridge, Massachusetts 02139

Attn:	Dr. R. Temkin/NW 14-4107	1 copy

Spectra Technologies
2755 Northup Way
Bellevue, Washington 98004

Attn:	Dr. J.M. Slater	1 copy

Mission Research Corporation
Suite 201
5503 Cherokee Avenue
Alexandria, Virginia 22312

Attn:	Dr. M. Bollen	1 copy
	Dr. Tom Hargreaves	1 copy

Mission Research Corporation
1720 Randolph Road, S.E.
Albuquerque, New Mexico 87106

Attn:	Dr. Ken Busby	1 copy
	Mr. Brendan B. Godfrey	1 copy

SPAWAR
Washington, D.C. 20363

Attn:	E. Warden	
	Code PDE 106-3113	1 copy

Naval Research Laboratory

Addressee:	Attn: Name/Code	
Code 1001 -	T. Coffey	1 copy
CODE 1220 -	Security	1 copy
Code 2628 -	TID Distribution	22 copies
Code 4000 -	W. Ellis	1 copy
Code 4700 -	S. Ossakow	26 copies

Code 4700.1 - A.W. Ali	1 copy
Code 4710 - C. Kapetanakos	1 copy
Code 4740 - Branch Office	25 copies
Code 4740 - W. Black	1 copy
Code 4740 - A. Fliflet	1 copy
Code 4740 - S. Gold	1 copy
Code 4740 - A. Kinkead	1 copy
Code 4740 - W.M. Manheimer	1 copy
Code 4740 - M.E. Read	1 copy
Code 4740 - M. Rhinewine	1 copy
Code 4770 - G. Cooperstein	1 copy
Code 4790 - B. Hui	1 copy
Code 4790 - C.M. Hui	1 copy
Code 4790 - Y.Y. Lau	1 copy
Code 4790 - P. Sprangle	1 copy
Code 5700 - L.A. Cosby	1 copy
Code 6840 - S.Y. Ahn	1 copy
Code 6840 - A. Ganguly	1 copy
Code 6840 - R.K. Parker	1 copy
Code 6840 - N.R. Vanderplaats	1 copy
Code 6850 - L.R. Whicker	1 copy
Code 6875 - R. Wagner	1 copy

Naval Sea Systems Command
Department of the Navy
Washington, D.C. 20362
Attn: Commander George Bates
PMS 405-300 — 1 copy

Northrop Corporation
Defense Systems Division
600 Hicks Rd.
Rolling Meadows, Illinois 60008
Attn: Dr. Gunter Dohler — 1 copy

Oak Ridge National Laboratory
P.O. Box Y
Mail Stop 3
Building 9201-2
Oak Ridge, Tennessee 37830
Attn: Dr. A. England — 1 copy

Office of Naval Research
800 N. Quincy Street
Arlington, Va. 22217
Attn: Dr. C. Roberson — 1 copy
Dr. W. Condell — 1 copy
Dr. T. Berlincourt — 1 copy

Office of Naval Research
1030 E. Green Street
Pasadena, CA 91106
Attn: Dr. R. Behringer — 1 copy

Optical Sciences Center
University of Arizona
Tucson, Arizona 85721
Attn: Dr. Willis E. Lamb, Jr. — 1 copy

OSD/SDIO
Attn: IST (Dr. H. Brandt)
Washington, D.C. 20301-7100 — 1 copy

Pacific Missile Test Center
Code 0141-5
Point Muga, California 93042
Attn: Will E. Chandler — 1 copy

Physical Dynamics, Inc.
P.O. Box 10367
Oakland, California 94610
Attn: A. Thomson — 1 copy

Physics International
2700 Merced Street
San Leandro, California 94577
Attn: Dr. J. Benford — 1 copy

Princeton Plasma
Plasma Physics Laboratory
James Forrestal Campus
P.O. Box 451
Princeton, New Jersey 08544
Attn: Dr. H. Hsuan — 2 copies
Dr. J. Doane — 1 copy

Quantum Institute
University of California
Santa Barbara, California 93106
Attn: Dr. L. Elias — 1 copy

Raytheon Company
Microwave Power Tube Division
Foundry Avenue
Waltham, Massachusetts 02154
Attn: N. Dionne — 1 copy

Sandia National Laboratories
ORG. 1231, P.O. Box 5800
Albuquerque, New Mexico 87185
Attn: Dr. Thomas P. Wright — 1 copy
Mr. J.E. Powell — 1 copy
Dr. J. Hoffman — 1 copy
Dr. W.P. Ballard — 1 copy
Dr. C. Clark — 1 copy

Science Applications, Inc.
1710 Goodridge Dr.
McLean, Virginia 22102
Attn: Adam Drobot — 1 copy
P. Vitrello — 1 copy

Stanford University
High Energy Physics Laboratory
Stanford, California 94305
Attn: Dr. T.I. Smith — 1 copy

TRW, Inc.
Space and Technology Group
Suite 2600
1000 Wilson Boulevard
Arlington, VA 22209
Attn: Dr. Neil C. Schoen — 1 copy

TRW, Inc.
Redondo Beach, California 90278
Attn: Dr. H. Boehmer — 1 copy
Dr. T. Romisser — 1 copy

University of California
Physics Department
Irvine, California 92717
Attn: Dr. G. Benford — 1 copy
Dr. N. Rostoker — 1 copy

University of California
Department of Physics
Los Angeles, CA 90024
Attn: Dr. A.T. Lin — 1 copy
Dr. N. Luhmann — 1 copy
Dr. D. McDermott — 1 copy

University of Maryland
Department of Electrical Engineering
College Park, Maryland 20742
Attn: Dr. V. L. Granatstein — 1 copy
Dr. W. W. Destler — 1 copy

University of Maryland
Laboratory for Plasma and Fusion
Energy Studies
College Park, Maryland 20742
Attn: Dr. Jhan Varyan Hellman — 1 copy
Dr. John McAdoo — 1 copy
Dr. John Finn — 1 copy
Dr. Baruch Levush — 1 copy
Dr. Tom Antonsen — 1 copy
Dr. Edward Ott — 1 copy

University of Tennessee
Dept. of Electrical Engr.
Knoxville, Tennessee 37916
Attn: Dr. I. Alexeff — 1 copy

University of New Mexico
Department of Physics and Astronomy
800 Yale Blvd, N.E.
Albuquerque, New Mexico 87131
Attn: Dr. Gerald T. Moore — 1 copy

University of Utah
Deparment of Electrical Engineering
3053 Merrill Engineering Bldg.
Salt Lake City, Utah 84112
Attn: Dr. Larry Barnett — 1 copy
Dr. J. Mark Baird — 1 copy

U. S. Naval Academy
Annapolis, Maryland 21402-5021 — 1 copy

U. S. Army
Harry Diamond Labs
2800 Powder Mill Road
Adelphi, Maryland 20783-1145
Attn: Dr. Edward Brown — 1 copy
Dr. Michael Chaffey — 1 copy

Varian Associates
611 Hansen Way
Palo Alto, California 94303
Attn: Dr. H. Jory — 1 copy
Dr. David Stone — 1 copy
Dr. Kevin Felch — 1 copy
Dr. A. Salop — 1 copy

Yale University
Applied Physics
Madison Lab
P.O. Box 2159
Yale Station
New Haven, Connecticut 06520
Attn: Dr. N. Ebrahim — 1 copy
Dr. I. Bernstein — 1 copy

END

11-87

DTIC